

ENVIRONMENTAL ASPECTS OF TWO TORNADO OUTBREAKS ASSOCIATED WITH LANDFALLING TROPICAL CYCLONES

Justin D. Lane*

NOAA/NWS Weather Forecast Office, Greer, SC

1. Introduction.

For many years, meteorologists have recognized that landfalling tropical cyclones (LTCs) are capable of altering the on-shore synoptic and mesoscale environments in such a manner that the potential for tornadoes increases in advance of the cyclone. Gentry (1983) observed that vertical wind shear increased substantially over land, as surface drag led to reduced wind speeds near the ground, while winds above the friction layer remained quite strong. McCaul (1991) found that environmental helicity in the right front quadrant of LTCs was often quite large. Novlan and Gray (1974) identified the centroid of LTC-related tornadoes at a radius of 240 km northeast of the cyclone center. The results of numerical simulations by McCaul and Weisman (1996) revealed that individual cells within the outer rain bands of LTCs often exhibit characteristics similar to Great Plains supercell thunderstorms, despite the much weaker potential buoyancy that typifies LTC environments.

Recently, Vescio et al. (1996) and Curtis (2004) have speculated on the role of mid-level dry air intrusions in LTC-related tornado outbreaks. Curtis found that 11 of the 13 “outbreak” cases that he identified since 1960 have been closely linked with large gradients of relative humidity in the 700-500 hPa layer. The numerical modeling study of Romine and Wilhelmson (2002) confirmed that the vertical vorticity of simulated thunderstorms in tropical

environments increased when mid-level dry air was introduced to the modeled atmosphere.

This paper focuses on several aspects of two LTCs, each responsible for historic outbreaks of tornadoes during September 2004 in the southeast and mid-Atlantic regions of the United States. The purpose of the study is to assist operational forecasters in identifying environmental characteristics associated with LTCs that may be conducive to large outbreaks of tornadoes. In addition, comparisons are made between the two outbreaks analyzed in this study, and in previous studies of LTC-related tornado outbreaks. Section 2 discusses the background and some of the environmental aspects of the Tropical Storm Frances outbreak, focusing in particular on tornadoes that occurred in the Midlands of South Carolina. Section 3 provides a discussion of the mesoscale environment of tornadoes that occurred in the Upper Savannah River Valley in association with the remnants of Hurricane Ivan. The final section will offer a discussion and some conclusions.

2. Tornado Outbreak Associated with Tropical Cyclone Frances

a. Background

Hurricane Frances made landfall between Ft. Pierce and West Palm Beach, FL at 0500 UTC on 5 September 2004. Frances weakened to a tropical storm as it moved across the Florida Peninsula before emerging over the northeast Gulf of Mexico and making

* *Corresponding author address:* Justin Lane, NOAA, National Weather Service, 1549 GSP Dr, Greer, SC 29651; e-mail: justin.lane@noaa.gov

landfall again near Panama City, FL at 1800 UTC on 6 September 2004. The remnant circulation weakened rapidly as it moved across western Georgia and eventually over the southern and central Appalachians. A total of 96 tornadoes occurred from 2100 UTC 4 September through 2000 UTC 8 September 2004 in association with Frances across the southeast and the Mid-Atlantic regions. This is one of the largest LTC-related outbreaks in history (Table 1). Forty-five events occurred in South Carolina alone: the largest tornado outbreak in state history.

As Frances weakened over southwest Georgia, convection around the center of the circulation began to diminish rapidly (not shown). By 0600 UTC on 7 September 2004, the strongest convection was displaced approximately 240 km north to 320 km east of the center of circulation. This placed the outermost rain bands associated with the cyclone across the coastal plain of South Carolina.

Between 0700 UTC and 1900 UTC, as rain bands continuously developed and moved north and northwest over portions of the Carolinas and Georgia, 32 tornadoes were reported (enclosed red dashed-dotted area in Fig. 1). All of these events occurred within the right front quadrant (RFQ) of the cyclone, between 350 and 500 km from the center of circulation. Almost all of these tornadoes occurred in the Midlands and coastal plain of South Carolina.

b. Analysis of Environmental Data

At 0600 UTC, surface analysis (not shown) revealed weak cold air damming, marked by the presence of an inverted ridge and northeast flow, was evident across inland areas of the Mid-Atlantic, the Carolinas, and northeast Georgia. At the leading edge of this ridge, a weak baroclinic boundary, separating the damming region from a slightly warmer maritime airmass, extended from the Carolina

coastal plain into central Georgia. By 1200 UTC, this boundary had moved inland, and was located across southern portions of the South Carolina Midlands (Fig. 1).

A sounding from the 0600 initialization of the Rapid Update Cycle (RUC) model (not shown), approximating the vertical structure of the atmosphere near Orangeburg, South Carolina (OGB) revealed the state of the atmosphere prior to the onset of the South Carolina outbreak. The surface-based convective available potential energy (SBCAPE) yielded by the sounding was approximately 680 J kg^{-1} . This value is less than the median CAPE from the Rasmussen and Blanchard (1998) baseline climatology of supercell parameters. However, it is comparable to the CAPE yielded by McCaul's (1991) composite of 86 observed LTC-related tornado soundings and the environmental profile utilized by McCaul and Weisman (1996) in their numerical simulations of supercells within an LTC environment.

The wind profile in the OGB sounding yielded a 0-3 km storm relative helicity (SRH) of $292 \text{ m}^2\text{s}^{-2}$. This value was similar to McCaul's sounding, and was higher than the median value calculated by Rasmussen and Blanchard for supercell environments. The OGB SRH was almost twice that of the McCaul and Weisman sounding.

The lifted condensation level (LCL) in the OGB sounding was 86 m AGL. While such a small value was typical of tropical environments, it has been hypothesized that tornadogenesis may be favored in environments characterized by low LCL heights (Markowski et al. 2002), assuming that wind shear and instability are adequate. The LCL height in the OGB sounding was much lower than the median height calculated by Craven and Brooks (2004) for significant tornadoes.

RUC analysis of 700 hPa relative humidity (RH) at 0600 UTC indicated RH values were generally 80 to 95% across the

outbreak area. However, there was an area of 50 to 70% RH (not shown) just off the coast of Georgia and South Carolina.

Although the instability present on 0600 UTC 7 September 2004 was not of a magnitude typically associated with large tornado outbreaks, helicity and LCL heights were well within the “significant tornado” category as identified in previous studies (Rasmussen and Blanchard, 1998; Craven and Brooks, 2004). This combination of environmental parameters was typical of the RFQ of LTCs. However, an unusually large number of tornadoes occurred across South Carolina during the subsequent 12 hours. A continued assessment of analysis data during the outbreak revealed how the environment underwent modification to become more favorable for tornadoes.

The sounding in Fig. 2, also from a point near OGB, was derived from the RUC analysis at 1200 UTC on 7 September 2004. This was the approximate time of peak tornadic activity across the South Carolina Midlands. The sounding, which best represented the atmospheric structure within the inflow region of the tropical rain bands, indicated that the atmosphere had undergone further destabilization, with SBCAPE of around 900 J kg^{-1} . This value was largely a result of the presence of a conditionally unstable layer in the 600 hPa to 500 hPa layer. This was in contrast to McCaul’s (1991) composite sounding, which revealed a deep layer of moist adiabatic lapse rates extending from approximately 600 hPa to the tropopause.

Coincident with the steep mid-level lapse rates is a layer of relatively dry air. The 1200 UTC RUC analysis of 700 hPa RH (Fig. 3) revealed that the area of <70% RH, evident off the Atlantic Coast at 0600 UTC, had advected onto the coastal plain by 1200 UTC. This introduction of drier air may have been the catalyst in steepening the lapse rates. Meanwhile, RH exceeded 90% across most of

Georgia at this time. This placed the outbreak area within this gradient of mid-level RH, consistent with the findings of Curtis (2004).

The sounding in Fig. 2 also indicated 0-3 km SRH remained high, at $286 \text{ m}^2\text{s}^{-2}$. The LCL height, which had increased to 135 m, was still quite favorable for tornado occurrence.

c. Radar Observations

Radar analysis between 0700 and 1900 UTC on 7 September 2004 indicated that most of the tornadic storms were either embedded within the outermost rain bands, or were relatively isolated from other convection (Fig. 4). In either case, almost all of the tornadic storms were oriented in such a way that there was little to no upstream convection to hinder inflow to their updrafts. As rain bands pivoted northward, and developed an east-west orientation, they became rather inactive in terms of tornado production as they became aligned with the low-level inflow vector.

Most of the tornadic storms during this period exhibited substantial low-level rotation (Fig. 5), as well as other supercell characteristics. Low-level mesocyclones were also quite long-lived, with some persisting for as much as 4.5 hours.

3. Tornado Outbreak Associated with Tropical Cyclone Ivan

a. Background

The eye of Hurricane Ivan came ashore just east of Mobile Bay in Alabama around 0700 UTC on 16 September 2004. The remnant circulation moved north across eastern Alabama, then along the western slopes of the southern Appalachians, before moving over Virginia and off the Atlantic Coast at around 1800 UTC on 18 September 2004. A total of 114 tornadoes were reported in association with Ivan from 1300 UTC 15

September 2004 to 2100 UTC 17 September 2004 across the southeast and Mid-Atlantic regions. This is the second largest LTC-related outbreak ever documented (Table 1.) A record of 25 tornadoes occurred in Georgia over a 30-hour period. All of these events occurred within the RFQ of the tropical cyclone.

b. Analysis of Environmental Data

Ivan was downgraded to a tropical storm at around 1300 UTC on 16 September 2004. At this time, the strongest convection was located near the center of circulation, across southern and central Alabama (not shown). Regional surface analysis at 1200 UTC 16 September (not shown) indicated weak cold air damming was in place across inland portions of the Carolinas, with a weak baroclinic boundary extending from the North Carolina coastal plain into central Georgia. This boundary moved slowly north during the day, and extended from the South Carolina Midlands into north central Georgia by 2100 UTC (Fig. 6).

A 1500 UTC sounding from the Local Analysis and Prediction System (LAPS) for a point near Athens, GA (not shown) revealed that the atmosphere over northeast Georgia was not conducive for strong convection. SBCAPE was approximately 360 J kg^{-1} . In addition, the sounding indicated that air parcels would have to overcome a convective inhibition (CIN) of 31 J kg^{-1} before reaching the level of free convection (LFC). Nevertheless, 0-3 km SRH was $194 \text{ m}^2\text{s}^{-2}$ and the LCL height 108 m, both favorable values for tornadoes. LAPS Analysis of 700 to 500 hPa RH (not shown) revealed a large area of <70% RH covered much of eastern Georgia and South Carolina, with a minimum value of around 50% over southeast Georgia.

At around 1700 UTC, strong rain bands began forming over central and eastern Georgia, approximately 250 km from the cyclone's center. Between 1900 UTC 16

September 2004 and 0000 UTC 17 September 2004, 20 tornadoes were reported in Georgia and western South Carolina (enclosed red dashed-dotted area in Fig. 6). These events were all located within the RFQ, between 240 and 500 km from the cyclone's center.

The 2100 UTC LAPS analysis sounding near AHN (Fig. 7) revealed how the atmosphere across northeast Georgia had evolved since 1500 UTC to one more favorable for strong convection. SBCAPE had increased to over 900 J kg^{-1} . Diurnal heating had eroded the CIN that was present earlier in the day. In addition, 0-3 km SRH was very large, at $350 \text{ m}^2\text{s}^{-2}$.

Another feature of the AHN sounding is the layer of relatively dry air in the mid-levels. This is also evident in Fig. 8, which indicated that RH of 50 to 55% had advected north into the Carolinas, while RH exceeded 90 percent across western Georgia and Alabama. This placed the outbreak region within this gradient (enclosed red dotted area in Fig. 6).

c. Radar Observations

Analysis of radar data from northeast Georgia and western South Carolina during this period of time revealed that most of the tornadic thunderstorms were embedded within the outermost rain bands (not shown), while others were associated with scattered convection that developed in advance of the bands (Fig. 9). Most of the tornadic storms exhibited supercell characteristics, including hook echoes (Fig. 9), and low-level rotational couplets (Fig. 10).

4. Discussion

These two historic cases provide further evidence to support the conclusions of Curtis (2004) and others that mid-level dry air intrusions play an important role in LTC-related tornado outbreaks. The advection of

drier air into the outbreak region can result in a steepening of mid-level lapse rates, and therefore an increase of SBCAPE, allowing for stronger updrafts to develop. Another important role that mid-level dry air could play in LTC-related outbreaks is through enhancement of available potential energy of thunderstorm downdrafts, which would result in stronger cold pools. The resultant increase in surface baroclinity suggests that horizontal vorticity will increase along the interface between the cold pool and thunderstorm inflow region. This vorticity can be tilted to the vertical by air flowing into the updraft, resulting in low-level mesocyclogenesis (Davies-Jones and Brooks 1993). The low LCL heights typical of LTC environments may subsequently promote the development of a warm rear flank downdraft (Markowski et al. 2002), which may be a necessary condition for tornadogenesis.

Perhaps as a direct result of the dry air, another characteristic shared by these two cases was the relatively strong instability that was present at the time of the outbreaks. Although SBCAPE at the height of both outbreaks was only around 900 J kg^{-1} , this value was larger than the CAPE yielded by McCaul's (1991) composite sounding. This implies that large LTC-related tornado outbreaks may be favored when values of CAPE are suggestive of a moderately unstable airmass (i.e., $\sim 1000 \text{ J kg}^{-1}$), as opposed to the weak potential buoyancy that typically accompanies tropical airmasses.

The presence of a pre-existing, weak baroclinic boundary is another characteristic shared by these two cases. It is unclear what role, if any, these boundaries played in the convective evolution during these events. However, it is interesting to note that in both cases, the outbreak region was located in proximity to a boundary. Figs. 1 and 6 indicate that a large portion of each outbreak area was located north of the boundary. Markowski et al. (1998) found that the "cool"

side of baroclinic surface boundaries may be a favored location for low level mesocyclogenesis, through the tilting of baroclinically generated horizontal vorticity by thunderstorm updrafts.

5. Conclusions

The tornadic events associated with the LTCs discussed in this paper further illustrate the importance of closely monitoring trends in environmental and radar data during an LTC event. A combination of high SRH, low LCL heights and instability conducive to tornado development is often observed in the RFQ. Forecasters should use available data sets to monitor shear and instability parameters in the RFQ to anticipate the possibility of tornadoes. The use of soundings from the RUC, LAPS, and other analysis packages are an efficient tool for forecasters to utilize in monitoring the evolution of the environment.

Forecasters should be especially cognizant of LTC environments that are characterized by CAPE values of $\sim 1000 \text{ J kg}^{-1}$ or more, as such environments may favor outbreaks of tornadoes. Large values of CAPE can develop via advection of drier air into the LTC environment. The potential for mid-level dry intrusions can be monitored through plan view analyses of RH in the 700-500 hPa layer from the RUC, LAPS, or other analysis packages. Areas within gradients of mid-level RH appear to be favored locations for LTC-related tornado outbreaks.

Acknowledgements: The author expresses his gratitude to Heather Hauser of NWS Eastern Region's Scientific Services Division, and Larry Lee, Science and Operations Officer, WFO Greer for their insightful comments.

References

Curtis, L., 2004: Midlevel dry intrusions as a factor in tornado outbreaks associated with landfalling tropical cyclones from

- the Atlantic and Gulf of Mexico. *Wea. Forecasting*, **19**, 411-427.
- Craven, J.P. and H.E. Brooks, 2004: Baseline climatology of sounding derived parameters associated with deep, moist convection. *Natl. Wea. Dig.* In press.
- Davies-Jones, R.P. and Brooks, H.E., 1993: Mesocyclogenesis from a theoretical perspective. The Tornado: Its Structure, Dynamics, Prediction, and Hazards, Geophys. Monogr., No. 79, Amer. Geophys. Union, 105-114.
- Gentry, R.C., 1983: Genesis of tornadoes associated with hurricanes. *Mon. Wea. Rev.*, **111**, 1793-1805.
- Markowski, P.M., E.N. Rasmussen, and J.M. Straka, 1998: The occurrence of tornadoes in supercells interacting with boundaries during VORTEX-95. *Wea. Forecasting*, **13**, 852-859.
- Markowski, P.M., J.M. Straka, and E.N. Rasmussen, 2002: Direct surface thermodynamic observations within the rear-flank downdrafts of nontornadic and tornadic supercells. *Mon. Wea. Rev.*, **130**, 1692-1721.
- McCaul, E.W., Jr., 1991: Buoyancy and shear characteristics of hurricane-tornado environments. *Mon. Wea. Rev.*, **119**, 1954-1978.
- McCaul, E.W., Jr., and M.L. Weisman, 1996: Simulations of shallow supercell storms in landfalling hurricane environments. *Mon. Wea. Rev.*, **124**, 408-429.
- Novlan, D.J., and W.M. Gray, 1974: Hurricane spawned tornadoes. *Mon. Wea. Rev.*, **102**, 476-488.
- Rasmussen, E.N. and D.O. Blanchard, 1998: A baseline climatology of sounding-derived supercell and tornado forecast parameters. *Wea. Forecasting*, **13**, 1148-1164.
- Romine, G., and R. Wilhelmson, 2002: Numerical investigation of the role of mid-level dryness on tropical mini-supercell behavior. Preprints, 21st Conf. *On Severe Local Storms*, San Antonio, TX, Amer. Meteor. Soc., 631-634.
- Vescio, M.D., S.J. Weiss, and F.P. Ostby, 1996: Tornadoes associated with Tropical Storm Beryl. *Natl. Wea. Dig.*, **1** (21), 2-10.

Table1. “Top 10” tornado outbreaks associated with tropical cyclones since 1960. Frances and Ivan numbers are still preliminary. (Adapted from Curtis, 2004.)

Storm (Year)	No. of tornadoes	F2 damage	F3 or greater	Deaths	Injuries
Allen (1980)	35	10	1	0	31
Andrew (1992)	56	1	1	2	49
Beryl (1994)	35	8	3	0	58
Beulah (1967)	117	5	6	5	41
Danny (1985)	42	9	5	1	63
David (1979)	34	13	2	2	31
Frances (2004)*	96	5	1	0	13
Georges (1998)	42	1	0	2	36
Gilbert (1988)	41	3	0	0	10
Ivan (2004)*	114	6	1	7	31

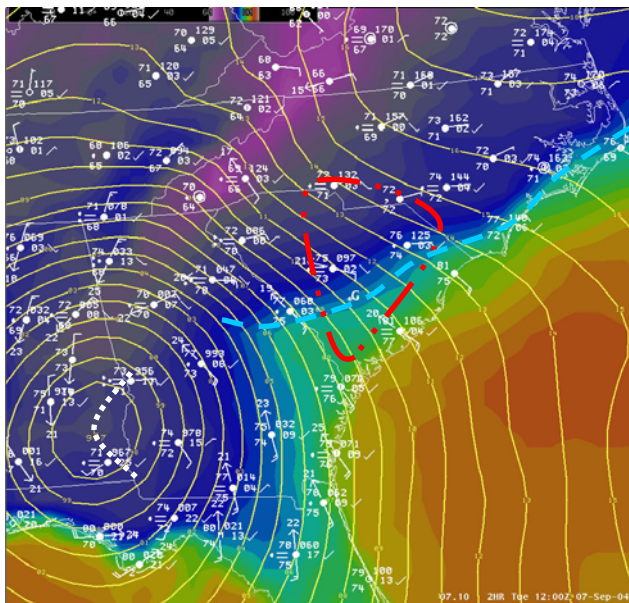


Figure 1. Surface analysis and METAR observations at 1200 UTC 7 September 2004. Solid (yellow) contours are sea level pressure analyzed every 2 hPa. The dashed (blue) line represents the approximate location of the surface boundary. The image is surface temperature (F). The dashed (white) line represents the track of the center of Frances between 0700 and 1900 UTC. The dotted-dashed (red) line denotes the area in which tornadoes were reported between 0700 and 1900 UTC.

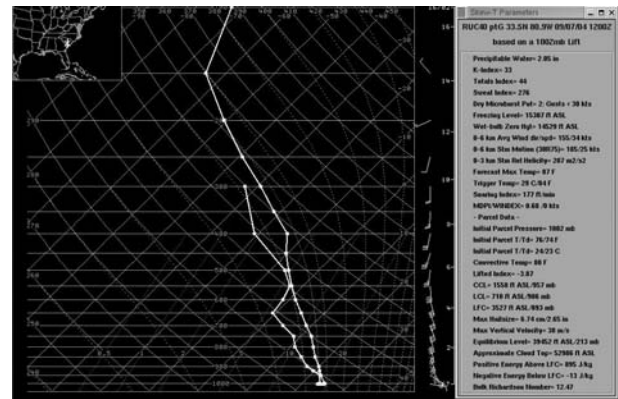


Figure 2. RUC sounding from Orangeburg, SC (OGB) at 1200 UTC on 7 September 2004.

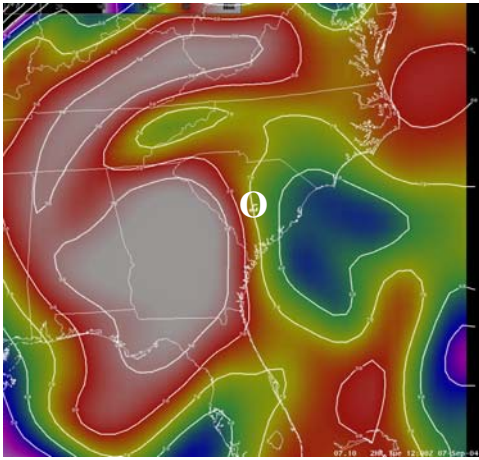


Figure 3. RUC analysis of 700 hPa relative humidity at 1200 UTC. Values in red are > 80%. Values in Blue are < 60%. "O" is the location of OGB.

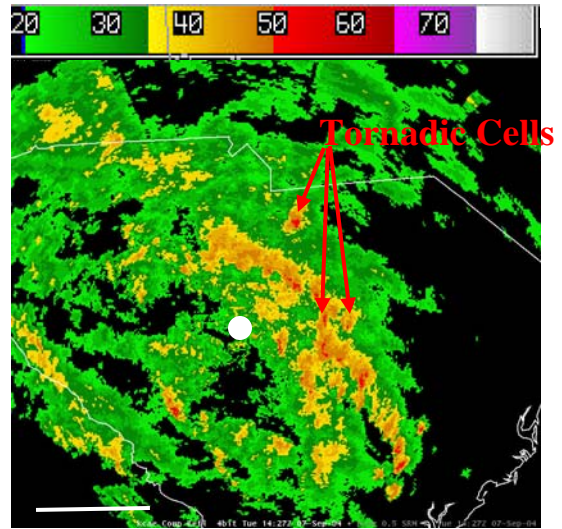


Figure 4. Composite reflectivity image from the Columbia, SC (CAE) WSR-88D at 1427 UTC on 7 September 2004. Cells that were previously tornadic, or later became tornadic are labeled. The scale at the top of the image is reflectivity in dBz. The line at the bottom left represents 50 km on the map. The white dot is the location of CAE.

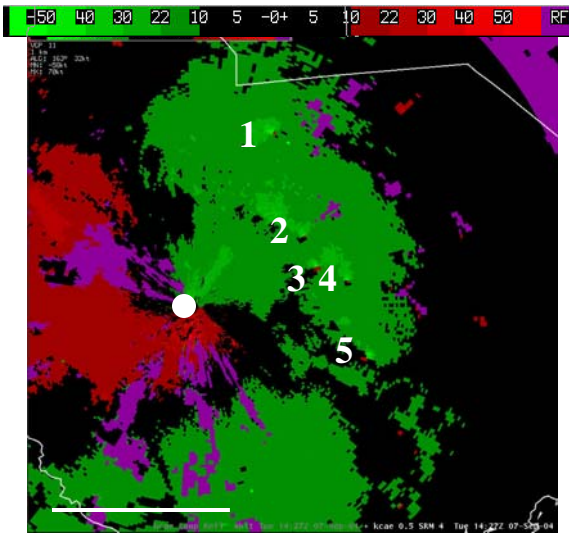


Figure 5. 0.5 degree storm relative velocity image from CAE WSR-88D at 1427 UTC on 7 September 2004. The scale above the image represents velocity in knots. Rotational couplets are labeled 1 through 5, with the numbers lying just to the left of each couplet. Couplets 1, 3, and 4 were associated with tornadoes within the hour prior to, or the hour after the time of this image.

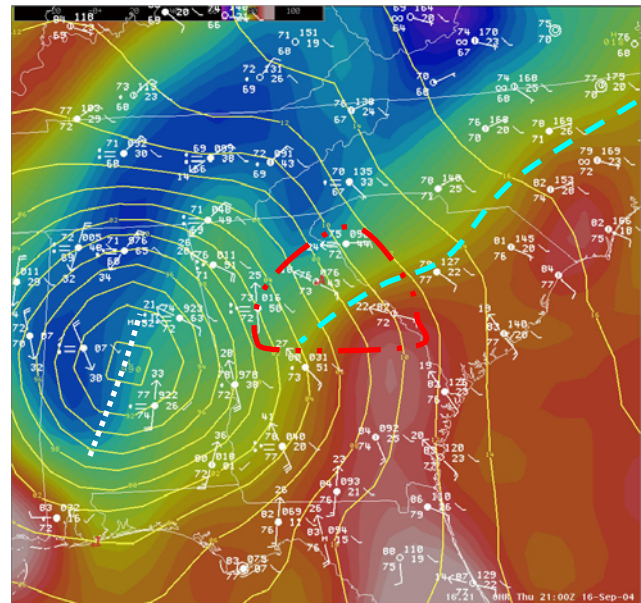


Figure 6. Same as in Fig. 1, except at 2100 UTC on 16 September 2004. Dashed (white) line is the track of Ivan between 1500 UTC September 16 and 0000 UTC September 17. Dashed-dotted (red) line denotes the area in which tornadoes were reported during this time.

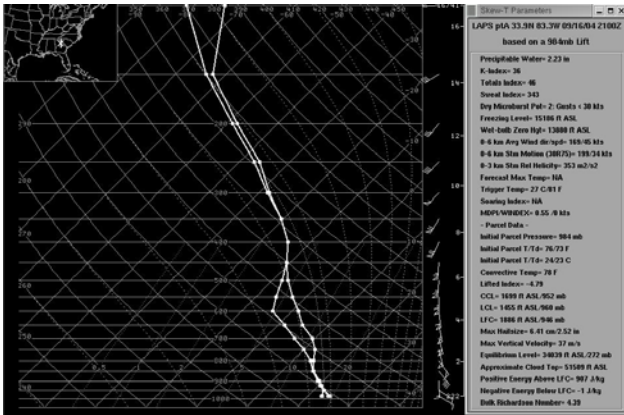


Figure 7. LAPS sounding from Athens, GA (AHN) at 2100 UTC on 16 September 2004.

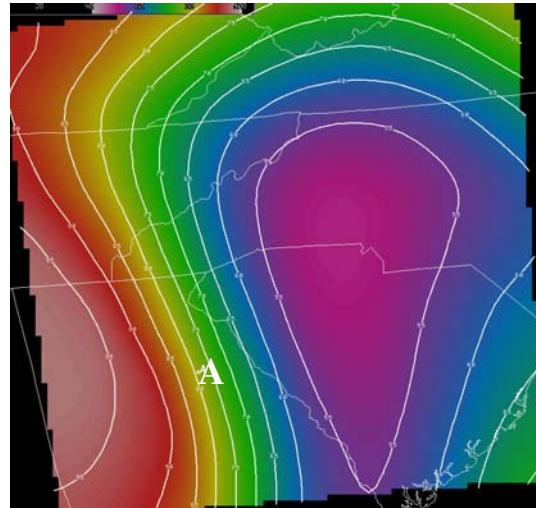


Figure 8. LAPS analysis of average 700 to 500 hPa relative humidity at 2100 UTC on 16 September 2004. Color scale is the same as in Fig. 3. Values in red are > 80%. “A” is the location of AHN.

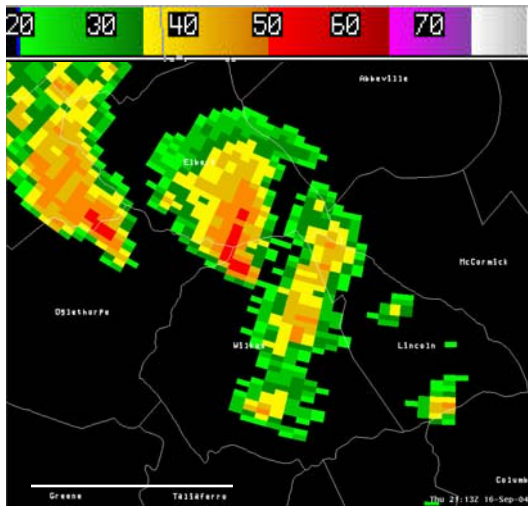


Figure 9. 0.5 degree reflectivity image from the Greer, SC (GSP) WSR-88D at 2113 UTC on 16 September 2004. The scale at the top of the image is reflectivity in dBz. The solid line at the bottom left represents a distance of 25 km on this map. County names are indicated.

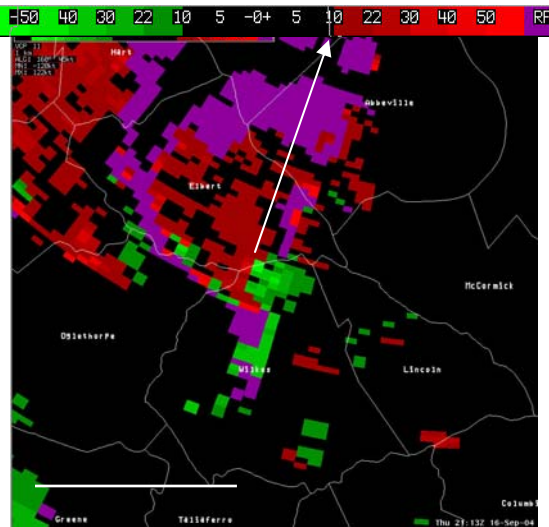


Figure 10. 0.5 degree storm relative velocity image from GSP at 2113 UTC on 16 September 2004. The scale above the image represents velocity in knots. The white arrow points toward the location of GSP. The circulation located near the origin of the arrow is around 78 km from the radar. County names are indicated.